DMD Fast Forward. Published on January 14, 2021 as DOI: 10.1124/dmd.120.000126
This article has not been copyedited and formatted. The final version may differ from this version.

Title page

In vitro evidence of potential interactions between CYP2C8 and candesartan acyl-β-D-glucuronide in the liver

Yurie Katsube, Masayuki Tsujimoto, Hiroyoshi Koide, Daiki Hira, Yoshito Ikeda, Tetsuya Minegaki, Shin-ya Morita, Tomohiro Terada, and Kohshi Nishiguchi

Department of Clinical Pharmacy, Kyoto Pharmaceutical University, Kyoto, Japan (YK[#], MT, HK[*], TM, and KN)

[#]*Present address: Department of Pharmacy, Kyushu University Hospital, Fukuoka, Japan*

[*]*Present address: Department of Pharmacy, Shiga University of Medical Science Hospital, Shiga, Japan*

Department of Pharmacy, Shiga University of Medical Science Hospital, Shiga, Japan (DH, YI[$], TM, SM, and TT)

[$]*Present addr*ess: *Laboratory of Medicinal Cell Biology, Kobe Pharmaceutical University, Kobe, Japan*

College of Pharmaceutical Sciences, Ritsumeikan University, Shiga, Japan (DH)

DMD Fast Forward. Published on January 14, 2021 as DOI: 10.1124/dmd.120.000126
This article has not been copyedited and formatted. The final version may differ from this version.

Running title page

Running title:

Candesartan glucuronide serves as a CYP2C8 inhibitor

Corresponding author:

Dr. Masayuki Tsujimoto

Kyoto Pharmaceutical University,

5 Misasagi nakauchi-cho, Yamashina-ku, Kyoto 607-8414, Japan

E-mail: tsujimt@mb.kyoto-phu.ac.jp

Tel: +81-75-595-4628

Number of text pages: 36

Number of tables: 1

Number of figures: 8

Number of references: 54

Number of words (Abstract): 226

Number of words (Introduction): 614

Number of words (Discussion): 1541

Abbreviations:

CYP, cytochrome P450

DCF, 2′,7′-dichlorofluorescein

DMEM, Dulbecco's modified Eagle's medium

FL, fluorescein

G6P, glucose-6-phosphate

G6PDH, glucose-6-phosphate dehydrogenase

DMD Fast Forward. Published on January 14, 2021 as DOI: 10.1124/dmd.120.000126
This article has not been copyedited and formatted. The final version may differ from this version.

HBSS, Hank’s balanced salt solution

HEK, human embryonic kidney

HLMs, human liver microsomes

HPLC, high-performance liquid chromatography

OATP, organic anion-transporting polypeptide

PBS, phosphate-buffered saline

TC, paclitaxel plus carboplatin combination

UDPGA, UDP-glucuronic acid

UGT, UDP-glucuronosyltransferase

DMD Fast Forward. Published on January 14, 2021 as DOI: 10.1124/dmd.120.000126
This article has not been copyedited and formatted. The final version may differ from this version.

Abstract

Growing evidence suggests that certain glucuronides function as potent inhibitors of cytochrome P450 (CYP) 2C8. We previously reported the possibility of drug–drug interactions between candesartan cilexetil and paclitaxel. In this study, we evaluated the effects of candesartan *N*2-glucuronide and candesartan acyl-β-D-glucuronide on pathways associated with the elimination of paclitaxel, including those involving organic anion-transporting polypeptide (OATP) 1B1, OATP1B3, CYP2C8, and CYP3A4. UDP-glucuronosyltransferase (UGT) 1A10 and UGT2B7 were found to increase candesartan *N*2-glucuronide and candesartan acyl-β-D-glucuronide formation in a candesartan concentration-dependent manner. Additionally, the uptake of candesartan *N*2-glucuronide and candesartan acyl-β-D-glucuronide by cells stably expressing OATPs is a saturable process with a K_m of 5.11 and 12.1 μM for OATP1B1 and 28.8 and 15.7 μM for OATP1B3, respectively; both glucuronides exhibit moderate inhibition of OATP1B1/1B3. Moreover, the hydroxylation of paclitaxel was evaluated using recombinant CYP3A4 and CYP3A5. Results show that candesartan, candesartan *N*2-glucuronide, and candesartan acyl-β-D-glucuronide inhibit the CYP2C8-mediated metabolism of paclitaxel, with candesartan acyl-β-D-glucuronide exhibiting the strongest inhibition (the 50% inhibitory concentration (IC_{50}) is 18.9 μM for candesartan acyl-β-D-glucuronide, 150 μM for candesartan, and 166 μM for candesartan *N2*-glucuronide). However, time-dependent inhibition of CYP2C8 by candesartan acyl-β-D-glucuronide was not observed. Conversely, the IC_{50} values of all the compounds are comparable for CYP3A4. Taken together, these data suggest that candesartan acyl-β-D-glucuronide is actively transported by OATPs into hepatocytes, and drug–drug interactions may occur with coadministration of candesartan and CYP2C8 substrates including paclitaxel as a result of the inhibition of CYP2C8 function.

DMD Fast Forward. Published on January 14, 2021 as DOI: 10.1124/dmd.120.000126
This article has not been copyedited and formatted. The final version may differ from this version.

Significance Statement

This study demonstrates that the acyl glucuronidation of candesartan to form candesartan acyl-β-D-glucuronide enhances CYP2C8 inhibition while exerting minimal effects on CYP3A4, OATP1B1, and OATP1B3. Thus, candesartan acyl-β-D-glucuronide might represent a potential mediator of drug–drug interactions between candesartan and CYP2C8 substrates, such as paclitaxel, in clinical settings. This work adds to the growing knowledge regarding the inhibitory effects of glucuronides on CYP2C8.

DMD Fast Forward. Published on January 14, 2021 as DOI: 10.1124/dmd.120.000126
This article has not been copyedited and formatted. The final version may differ from this version.

Introduction

Glucuronidation of drugs is involved in their detoxification in mammals. Acyl glucuronides have been reported as inducers of toxicity owing to their high chemical reactivity, which, for example, causes acylation and glycation of proteins, resulting in their covalent binding to proteins (Lassila et al., 2015). Some acyl glucuronides can interact with cytochrome P450 (CYP) isoforms. In particular, growing evidence suggests that some glucuronides are potent inhibitors of CYP2C8, an important enzyme involved in drug metabolism (Backman et al., 2015; Tornio et al., 2017). In fact, the role of glucuronides in drug–drug interactions via CYP2C8 has been recognized for combination therapy with cerivastatin and gemfibrozil (Chang et al., 2004). However, severe myopathy and rhabdomyolysis result from drastically altered pharmacokinetics of cerivastatin (Backman et al., 2002) due to potent inhibition of CYP2C8 by gemfibrozil acyl-β-D-glucuronide (Backman et al., 2002; Wang et al., 2002; Ogilvie et al., 2006; Takagi et al., 2015; Varma et al., 2015). Similarly, coadministration of clopidogrel with repaglinide induces an approximately 2.5–5.1-fold increase in the area under the plasma concentration–time curve (AUC) of repaglinide (Tornio et al., 2014), which is a substrate of CYP2C8 and organic anion-transporting polypeptide (OATP) 1B1, a hepatic uptake transporter (Kajosaari et al., 2005; Gertz et al., 2014). Orally administered clopidogrel is hydrolyzed to clopidogrel carboxylic acid and subsequently converted to clopidogrel acyl-β-D-glucuronide (Farid et al., 2010), which is a strong, time-dependent inhibitor of CYP2C8 and a weak inhibitor of OATP1B1 that is considered to be responsible for the interaction between repaglinide and clopidogrel (Tornio et al., 2014). Besides gemfibrozil and clopidogrel, numerous other drug substrates have been described for glucuronosyltransferases; however, the CYP2C8 inhibitory effects of other glucuronides remain unknown.

Following intravenous administration, paclitaxel is transported to hepatocytes by OATP1B1 and OATP1B3, where it becomes metabolized to 6α-hydroxypaclitaxel and *p*-3′-hydroxypaclitaxel by CYP2C8 and to a lesser extent by CYP3A4, respectively (Fujino et al., 2001; Cresteil et al., 2002). Agergaard et al. (2017) reported that concomitant use of clopidogrel aggravated paclitaxel-induced neuropathy in patients, thereby confirming that

DMD Fast Forward. Published on January 14, 2021 as DOI: 10.1124/dmd.120.000126
This article has not been copyedited and formatted. The final version may differ from this version.

coadministration of paclitaxel with medications exerting CYP2C8 inhibitory effects results in severe adverse events caused by drug–drug interactions.

Previously, we performed a comprehensive retrospective analysis of concomitant medications to identify potential risk factors for chemotherapy-induced severe neutropenia in patients administered paclitaxel plus carboplatin combination (TC) therapy. We found that concomitant use of candesartan cilexetil, unlike that of other angiotensin receptor blockers, could result in severe neutropenia (Katsube et al., 2018). Candesartan cilexetil, an angiotensin II receptor blocker, is commonly administered for the treatment of hypertension. Almost all candesartan cilexetil is hydrolyzed to candesartan in the gastrointestinal tract (Yamaoka et al., 1981). However, previous *in vitro* studies have shown that the inhibitory effects of candesartan on CYP2C8/CYP3A4 and OATPs are not sufficiently strong to suggest an interaction with paclitaxel at clinically relevant concentrations (Taavitsainen et al., 2000; Senda et al., 2015; van de Steeg et al., 2015). Following oral administration of candesartan to rats and dogs, candesartan acyl-β-D-glucuronide and candesartan *N*2-glucuronide were detected in the feces and blood (Kondo et al., 1996), respectively (Fig. 1). In addition, glucuronidation of candesartan by human UDP-glucuronosyltransferase (UGT) yields two metabolites, identified as *O*-glucuronide and tetrazole-*N*2-glucuronide, when candesartan is incubated with human liver microsomes (HLMs) or with individual human UGTs (Alonen et al., 2008). However, no definitive *in vitro* proof of interactions between candesartan glucuronides and the paclitaxel hepatic elimination pathways, including those involving OATPs and CYPs, has been presented.

The objective of the present study was, therefore, to investigate the possible interactions of candesartan and candesartan glucuronides with CYP2C8. We also sought to determine whether candesartan glucuronides serve as substrates of OATPs, and as inhibitors of CYP2C8, CYP3A4, and OATPs *in vitro*.

DMD Fast Forward. Published on January 14, 2021 as DOI: 10.1124/dmd.120.000126
This article has not been copyedited and formatted. The final version may differ from this version.

Materials and methods

Materials

Paclitaxel and glucose-6-phosphate dehydrogenase (G6PDH) were purchased from Wako Pure Chemical Industries (Osaka, Japan). β-$NADP^+$ and glucose-6-phosphate (G6P) were purchased from Oriental Yeast Co. (Tokyo, Japan). Docetaxel trihydrate, 2′,7′-dichlorofluorescein (DCF), and fluorescein (FL) were purchased from Tokyo Chemical Industry (Tokyo, Japan). Candesartan was purchased from LKT Laboratories, Inc. (St. Paul, MN, USA). Candesartan *N*2-glucuronide, candesartan acyl-β-D glucuronide, and 6α-hydroxypaclitaxel were purchased from Toronto Research Chemicals (North York, ON, Canada). HLMs were purchased from BD Biosciences (Woburn, MA, USA). These HLMs were pooled from 21 individuals (14 males and 7 females). Human recombinant CYP2C8 and CYP3A4 were purchased from Cypex (Dundee, UK). *p*-3′-Hydroxypaclitaxel and human recombinant UGT1A10 and UGT2B7 were purchased from Corning (Corning, NY, USA). UDP-glucuronic acid (UDPGA) was purchased from Yamasa Co. (Tokyo, Japan).

Cells

Previously established OATP1B1-transfected human embryonic kidney (HEK) 293 (HEK/OATP1B1) cells and empty vector-transfected HEK293 (HEK/Mock) cells (Katsube et al., 2017) were used in this study. OATP1B3-transfected HEK293 (HEK/OATP1B3) cells were kindly provided by Prof. Hiroyuki Kusuhara and Dr. Kazuya Maeda (Laboratory of Molecular Pharmacokinetics, Tokyo University, Japan). HEK/OATP1B1, HEK/OATP1B3, and HEK/Mock cells were maintained in Dulbecco's modified Eagle's medium (DMEM; Life Technologies, Grand Island, NY, USA), supplemented with 10% (v/v) fetal bovine serum (Thermo Fisher Scientific, Waltham, MA, USA), 100 U/mL penicillin, 100 μg/mL streptomycin (Nakalai Tesque, Kyoto, Japan), 0.1 mM non-essential amino acids (Nakalai Tesque), and 0.72 mM geneticin (Nakalai Tesque), in an atmosphere of 5% CO_2 in a humidified incubator at 37

DMD Fast Forward. Published on January 14, 2021 as DOI: 10.1124/dmd.120.000126
This article has not been copyedited and formatted. The final version may differ from this version.

°C.

For cellular uptake experiments, cells were seeded in collagen-coated 48-well (0.4×10^5 cells/well) or 24-well (0.8×10^5 cells/well) plates (Corning). The cells were cultured in DMEM in a humidified atmosphere with 5% CO_2 at 37 °C. After 3 days, the medium was replaced with DMEM containing 5 mM sodium butyrate, a histone deacetylase inhibitor, to enhance gene expression (Kondo et al., 1996). On the next day, the intracellular uptake experiments described below were performed.

Inhibition of OATP1B1 and OATP1B3 activity

The intracellular uptake experiments were performed as previously described (Katsube et al., 2017), with DCF and FL used as OATP1B1 and OATP1B3 substrates, respectively (De Bruyn et al., 2011; Koide et al., 2017). The cells were washed twice with warmed HEPES–Hank's balanced salt solution (HBSS; 137 mM NaCl, 5.4 mM KCl, 1.3 mM $CaCl_2$, 0.4 mM $MgSO_4$, 0.5 mM $MgCl_2$, 0.3 mM Na_2HPO_4, 0.4 mM KH_2PO_4, 4.2 mM $NaHCO_3$, 5.6 mM glucose, and 25.0 mM HEPES, pH 7.4) and then preincubated for 10 min at 37 °C in HEPES–HBSS buffer. After aspiration of the HEPES–HBSS buffer, the uptake assay was initiated by the addition of 0.2 mL of warmed HEPES–HBSS buffer containing the substrate (1 μM DCF or 3 μM FL), with or without the test compound (candesartan, candesartan *N*2-glucuronide, or candesartan acyl-β-D-glucuronide) at concentrations of 1 and 10 μM. The uptake assay was terminated by removing the uptake buffer, 3 min after initiation, and the cells were subsequently washed three times with ice-cold phosphate-buffered saline (PBS) containing 0.5 mM $MgCl_2$ and 1 mM $CaCl_2$.

To quantify the intracellular accumulation of DCF and FL, the cells were lysed with 150 μL of 0.1 M NaOH. To normalize the data to cell numbers, we measured the protein content using the Lowry protein assay with bovine serum albumin as the standard (Lowry et al. 1951). FL and DCF were quantified as described previously (Koide et al., 2017). Briefly, 100 μL of each sample was transferred to a 96-well solid black polystyrene plate (Corning), and

DMD Fast Forward. Published on January 14, 2021 as DOI: 10.1124/dmd.120.000126
This article has not been copyedited and formatted. The final version may differ from this version.

quantification was carried out by measuring the fluorescence intensity (excitation at 490 nm; emission at 515 nm) using a microplate reader (Power Scan® HT; BioTek Japan, Tokyo, Japan).

Intracellular glucuronide uptake mediated by OATP1B1 or OATP1B3

In the intracellular uptake experiments, HEK/OATP1B1 or HEK/OATP1B3 cells were washed twice with warmed HEPES–HBSS buffer and then preincubated for 10 min at 37 °C in HEPES–HBSS buffer. After aspiration of the HEPES–HBSS buffer, uptake was initiated via addition of warmed HEPES–HBSS buffer containing candesartan *N*2-glucuronide or candesartan acyl-β-D-glucuronide (0.5–30 μM). The uptake experiments were terminated by removal of the uptake buffer 3 min after initiation; the cells were then washed three times with ice-cold PBS containing 0.5 mM $MgCl_2$ and 1 mM $CaCl_2$.

To quantify the intracellular accumulation of glucuronides, cells were lysed with PBS containing 0.1% (w/v) Tween 20. The data were normalized to cell number, as described above and the glucuronides were quantified as described previously (Alonen et al., 2008). Briefly, 150 μL of acetonitrile containing 267 nM olmesartan as an internal standard (Ma et al., 2005), and 230 μL of 50 mM phosphate buffer (pH 3.0), were added to 110 μL of the sample. The mixture was vigorously vortexed for 1 min and centrifuged at 15,000 × *g* for 10 min, after which the upper layer was injected into an Inertsil ODS-III column (5 μm, 250 × 4.0 mm i.d.; GL Sciences, Inc., Tokyo, Japan), and the glucuronides were quantified using a high-performance liquid chromatography (HPLC) system equipped with a fluorescence detector (RF-20A; Shimadzu, Kyoto, Japan) by measuring fluorescence intensity (excitation at 260 nm; emission at 395 nm). For HPLC, the flow rate of the mobile phase, comprising 50 mM phosphate buffer (pH 3.0) and acetonitrile (70:30, v/v), was 1.0 mL/min.

Glucuronidation of candesartan by recombinant human UGT1A10 and UGT2B7

Relatively high levels of *O*-glucuronidation, corrected for the expression of individual human recombinant UGTs, were obtained, with the highest levels observed for UGT1A10 followed by UGT1A7–1A9. In addition, relatively high levels of *N*2-glucuronidation were

DMD Fast Forward. Published on January 14, 2021 as DOI: 10.1124/dmd.120.000126
This article has not been copyedited and formatted. The final version may differ from this version.

obtained using UGT1A3 and UGT2B7 when candesartan and recombinant protein were incubated for 4 h at concentrations of 1 mM and 1.0 mg protein/mL, respectively (Alonen et al., 2008). Thus, candesartan glucuronidation was assessed using human recombinant UGT1A10 and UGT2B7 as described previously (Alonen et al., 2008), with slight modifications. Each reaction mixture contained candesartan (0.5–30 μM) and 0.5 $mg \cdot mL^{-1}$ human recombinant UGT1A10 or UGT2B7, 27.5 $\mu g \cdot mL^{-1}$ alamethicin, and 50 mM phosphate buffer with 10 mM Mg^{2+} (pH 7.4). The reaction mixture was incubated at 37 °C for 5 min, and the reaction was initiated by the addition of 5 mM UDPGA. The mixture was incubated at 37 °C for another 60 min; thereafter, the reaction was terminated by the addition of acetonitrile. Glucuronides were quantified according to the method described above.

Inhibition of paclitaxel metabolism in human liver microsomes or recombinant human CYP2C8 and CYP3A4

Hydroxylation of paclitaxel was assessed using HLMs or human recombinant CYP2C8 and CYP3A4 as previously described (Wang et al., 2014; Tsujimoto et al., 2016), with minor modifications. Each reaction mixture contained 10 pmol/mL recombinant CYP2C8 or CYP3A4, with or without the test compounds (15.6–250 μM), in 50 mM phosphate buffer with 5 mM Mg^{2+} (pH 7.4). The CYP inhibition experiments were conducted as follows. a) Reversible inhibition: to determine the IC_{50} values of the test compounds by direct CYP inhibition, the reaction mixture was incubated at 37 °C for 5 min, after which the reaction was initiated by addition of the NADPH-regenerating system (5 mM G6P, 1.0 U/mL G6PDH, and 1 mM β-$NADP^{+}$) containing paclitaxel (2 μM). The mixture was then incubated at 37 °C for 30 min, and subsequently terminated by adding acetonitrile. b) IC_{50} shift assay: the time-dependent inhibition (TDI) of CYP was evaluated using the IC_{50} shift assay, which is the most commonly used assay for the assessment of TDI owing to its relative ease of execution in a drug discovery setting (Orr et al., 2012). To perform the IC_{50} shift assay, the reaction mixture (0.1 mg/mL HLMs, the NADPH-regenerating system, and a test compound in 50 mM phosphate buffer with 5 mM Mg^{2+}, pH 7.4) was incubated at 37 °C with the initial addition of the

DMD Fast Forward. Published on January 14, 2021 as DOI: 10.1124/dmd.120.000126
This article has not been copyedited and formatted. The final version may differ from this version.

NADPH-regenerating system for 30 min. The mixture was then added to a paclitaxel (2 μM)-containing solution and incubated for 10 min; the reaction was terminated by the addition of acetonitrile. c) K_i experiment: the K_i values for CYP2C8 were determined using the Dixon plot (no initial inhibition). Briefly, for direct CYP inhibition by the test compounds, the reaction mixture was incubated at 37 °C for 5 min, followed by initiation of the reaction by addition of the NADPH-regenerating system (5 mM G6P, 1.0 U/mL G6PDH, and 1 mM β-$NADP^+$) containing paclitaxel (0.5, 1.0, and 2.0 μM). The mixture was then incubated at 37 °C for 30 min, and the reaction was terminated by adding acetonitrile.

6α-hydroxypaclitaxel and 3′-*p*-hydroxypaclitaxel were quantified as described previously (Harris et al., 1994; Huizing et al., 1995). Briefly, 50 μL of acetonitrile containing 1 μM docetaxel as an internal standard (Garg and Ackland, 2000) and 3 mL of diethyl ether were added to a mixture containing the samples, and vigorously vortexed for 1 min. After centrifugation at 1,650 × *g* for 10 min, 2.8 mL of the upper layer was collected and evaporated to dryness under a stream of N_2 at 40 °C. The residue was then dissolved in the mobile phase (50 mM phosphate buffer, pH 7.0: acetonitrile, 55:45, v/v). The sample was injected into an HPLC system and quantified by measuring the absorbance at 229 nm using an Inertsil ODS-III column (5 μm, 250 × 4.0 mm i.d.) and a fluorescent detector (SPD-20A, Shimadzu).

Data analysis

The OATP1B1- or OATP1B3-mediated uptake of the glucuronides was calculated by subtracting the level of intracellular accumulation of the substrates in HEK/Mock cells from that in HEK/OATP1B1 or HEK/OATP1B3 cells. The data are presented as means ± standard deviation of the sample (SD) or as estimated means [95% confidence interval (CI)]. Significant differences between mean values were determined using the Student's *t*-test or one-way analysis of variance (ANOVA), followed by the Dunnett's test, and $p < 0.05$ was considered statistically significant.

The Michaelis–Menten constant (K_m) and maximum velocity (V_{max}) values, used as kinetic parameters of the OATP activity, were calculated using equations of the Michaelis–

DMD Fast Forward. Published on January 14, 2021 as DOI: 10.1124/dmd.120.000126
This article has not been copyedited and formatted. The final version may differ from this version.

Menten model (equation 2) to analyze the data with the MULTI program (Yamaoka et al., 1981). Equation (1) was used for HEK/OATP1B1 and HEK/OATP1B3 cells:

$$v = \frac{V_{max} \times [S]}{K_m \times [S]} + P_{dif} \times [S] \quad (1)$$

and equation (2) was used for HEK/Mock cells:

$$v = P_{dif} \times [S] \quad (2)$$

The substrate concentration at which the reaction rate was half of V_{max} (S_{50}) and maximum velocity (V_{max}) values, used as kinetic parameters of the UGT activity, was calculated using the Michaelis–Menten or the Hill equation (3) to analyze the data with the MULTI program (Yamaoka et al., 1981). The appropriate model was determined using the Eadie–Hofstee plot. When a bell-shaped curve was observed, the data were fitted using the Hill equation as this is characteristic of sigmoidal data (Madan et al., 2002).

$$v = \frac{V_{max} \times [S]^n}{S_{50}{}^n \times [S]^n} \quad (3)$$

where v, $[S]$, and n represent the initial glucuronidation velocity, the substrate concentration, and the Hill coefficient, respectively.

IC_{50} values of the test compound for the CYP2C8 or CYP3A4 activity were calculated using equation (4) to analyze the data with the MULTI program (Yamaoka et al., 1981):

$$I = 100 \times \left(1 - \frac{[I]^\gamma}{IC_{50}{}^\gamma + [I]^\gamma} \right) \quad (4)$$

where, I, $[I]$, and γ represent the inhibition of CYP activity (% of control), the concentration of the test compound, and a sigmoidal constant, respectively.

DMD Fast Forward. Published on January 14, 2021 as DOI: 10.1124/dmd.120.000126
This article has not been copyedited and formatted. The final version may differ from this version.

Results

Glucuronidation of candesartan to N2-glucuronide and acyl-β-D-glucuronide by recombinant UGT1A10 and UGT2B7

The concentration of candesartan *N*2-glucuronide was linearly increased by UGT1A10 and UGT2B7 in a candesartan concentration-dependent manner, up to 1 mM (Fig. 2). The kinetics of candesartan glucuronidation to candesartan acyl-β-D-glucuronide by UGT1A10 followed the sigmoidal autoactivation model, best fit with the Hill equation (Fig. 2C), which is demonstrated by a bell-shaped curve (Fig. 2C insets), whereas glucuronidation of candesartan to candesartan acyl-β-D-glucuronide by UGT2B7 followed the Michaelis–Menten model.

Uptake of glucuronides by HEK/OATP1B1 and HEK/OATP1B3 cells

The intracellular uptake of candesartan *N*2-glucuronide and candesartan acyl-β-D-glucuronide by HEK/OATP1B1 and HEK/OATP1B3 cells increased in a concentration-dependent manner and was significantly higher than the uptake by HEK/Mock cells. The OATP1B1- and OATP1B3-mediated uptake of candesartan glucuronide followed the Michaelis–Menten profile. Candesartan *N2*-glucuronide was transported by OATP1B1 (K_m = 5.11 μM), and to a smaller extent by OATP1B3 (K_m = 28.8 μM). The affinity of acyl glucuronide for OATP1B1 and OATP1B3 showed similar K_m values (K_m = 12.1 and 15.7 μM, respectively). The V_{max} values of OATP1B1 for acyl glucuronide and *N2*-glucuronide were 0.5 and 1.64 pmol·min^{-1}·mg protein^{-1}, respectively. The V_{max} values of OATP1B3 for acyl glucuronide and *N2*-glucuronide were 3.76 and 3.95 pmol·min^{-1}·mg protein^{-1}, respectively (Fig. 3).

Inhibitory effects of candesartan and its glucuronides on the uptake of OATP1B1 and OATP1B3 substrates

Candesartan and its glucuronides significantly inhibited the OATP1B1-mediated uptake of DCF and the OATP1B3-mediated uptake of FL in a concentration-dependent manner. OATP1B1- or OATP1B3-mediated uptake of each substrate was reduced by approximately

DMD Fast Forward. Published on January 14, 2021 as DOI: 10.1124/dmd.120.000126
This article has not been copyedited and formatted. The final version may differ from this version.

30-40% in the presence of 10 μM candesartan and candesartan acyl glucuronide compared to the control. In the presence of 10 μM candesartan *N2*-glucuronide, OATP1B1-mediated uptake of DCF was reduced by 66.7% compared to that in the control, whereas OATP1B3-mediated uptake of FL was only reduced by 36.3 (Fig. 4).

Inhibitory effects of candesartan and its glucuronides on the hydroxylation of paclitaxel by recombinant CYP2C8 and CYP3A4

Candesartan, candesartan *N*2-glucuronide, and candesartan acyl-β-D-glucuronide inhibited the CYP2C8-mediated metabolism of paclitaxel in a concentration-dependent manner. Moreover, candesartan acyl-β-D-glucuronide inhibited the metabolism more strongly (IC_{50} = 18.9 μM) than did candesartan (IC_{50} = 150 μM) or candesartan *N*2-glucuronide (IC_{50} = 166 μM) (Fig. 5A and Table 1). Candesartan (IC_{50} > 250 μM), candesartan *N*2-glucuronide (IC_{50} = 191 μM), and candesartan acyl-β-D-glucuronide (IC_{50} = 159 μM) also inhibited the CYP3A4-mediated metabolism of paclitaxel in a concentration-dependent manner (Fig. 5B and Table 1).

Inhibition models for candesartan and candesartan acyl-β-D-glucuronide

The importance of TDI and mechanism-based inhibition of CYP for accurate estimation of drug–drug interaction has been recognized. As shown in Fig. 6, since preincubation with NADPH did not shift the IC_{50} values of candesartan acyl-β-D-glucuronide, the K_i values for CYP2C8-mediated hydroxylation of paclitaxel were determined by direct inhibition (no initial inhibition). It is clear from the Dixon plot that the inhibition of CYP2C8 by candesartan was non-competitive (K_i = 133 ± 5.8 μM), whereas that by candesartan acyl-β-D-glucuronide was competitive (K_i = 7.12 ± 1.41 μM) (Fig. 7).

DMD Fast Forward. Published on January 14, 2021 as DOI: 10.1124/dmd.120.000126
This article has not been copyedited and formatted. The final version may differ from this version.

Discussion

Candesartan, candesartan *N*2-glucuronide, and candesartan acyl-β-D-glucuronide inhibited the CYP2C8- and CYP3A4-mediated metabolism of paclitaxel with candesartan acyl-β-D-glucuronide exhibiting the strongest inhibition of CYP2C8-mediated paclitaxel metabolism, without eliciting strong inhibition of CYP3A4 (Fig. 5 and Table 1). It is, therefore, important to monitor the substrates of CYP2C8, rather than of CYP3A4, that are used for treating patients administered candesartan.

Gemfibrozil acyl glucuronide (Ogilvie et al., 2006) and clopidogrel acyl glucuronide (Tornio et al., 2014) strongly inhibit CYP2C8 in a time- and metabolism-dependent manner. However, although candesartan acyl-β-D-glucuronide strongly inhibited CYP2C8 (Fig. 5), the IC_{50} shift assay did not show preincubation time-dependent inhibition of CYP2C8 (Fig. 6). Therefore, the mechanism of CYP2C8 inhibition by candesartan acyl-β-D-glucuronide differs from that of gemfibrozil acyl glucuronide and clopidogrel acyl glucuronide.

Moreover, candesartan noncompetitively inhibited CYP2C8 whereas candesartan acyl-β-D-glucuronide showed a strong competitive inhibition (Fig. 7) that was not time-dependent (Fig. 6). Kumar et al. (2002) reported that hydroxylation of diclofenac acyl glucuronide to 4′-hydroxy diclofenac acyl glucuronide, which is a major pathway responsible for metabolizing 30% of the *in vivo* dose (Stierlin et al., 1979), is primarily catalyzed by CYP2C8, not CYP3A4, CYP2C9, or CYP2D6, in the presence of NADPH and HLMs. Nishihara et al. (2012) revealed that sipoglitazar glucuronide becomes de-ethylated following incubation with HLMs, while CYP2C8 is predominantly involved in dealkylation. Although there are some reports that glucuronic acid conjugates serve as substrates for CYP2C8, incubation of 10 μM candesartan acyl-β-D-glucuronide with 10 pmol/mL CYP2C8 and the NADPH-regenerating system for 30 min did not induce degradation (Fig. S1). It is necessary to consider factors other than the affinity of CYP2C8 for the substrate binding site as the mechanism which candesartan acylglucuronide exhibits a CYP2C8 inhibitory effect. Jenkins et al. (2011) reported that multiple CYP2C8 inhibitors may contribute to the potent inhibitory effect of CYP2C8, but do not necessarily cause time-dependent inhibition by glucuronides

DMD Fast Forward. Published on January 14, 2021 as DOI: 10.1124/dmd.120.000126
This article has not been copyedited and formatted. The final version may differ from this version.

including gemfibrozil acyl glucuronide. In a comparative study using a docking simulator of certain gemfibrozil analogs in which the methyl group closest to heme was changed, they proposed that the presence or absence of a methyl group affects the time-dependent inhibition. Candesartan acyl-β-D-glucuronide contains a benzimidazole-7-carboxylate structure with glucuronized carboxylic acid. Candesartan cilexetil also contains a benzimidazole-7-carboxylate structure, and carboxylic acid is esterified with cilexetil (Fig. 1). Foti et al. (2016) reported that the degradation of candesartan cilexetil was minimal upon incubation with CYP2C8, with no appreciable formation of an ester-hydrolyzed product. Computational docking simulation showed that candesartan cilexetil strongly inhibited the CYP2C8-mediated amodiaquine metabolism (IC_{50} = 0.50 μM; Walsky et al., 2005), without interacting with the heme. Whether glucuronide conjugates can show more potent mechanism-based inhibition may not require that the glucuronides are a substrate for CYP2C8.

We show that not only UGT1A10, but also UGT2B7, produce candesartan acyl-β-D glucuronide (Fig. 2). Most reports on candesartan metabolism do not mention glucuronidation as a metabolic pathway because in a phase I clinical trial in which candesartan cilexetil was administered to healthy subjects, only candesartan and its main oxidized metabolites were detected (Kondo et al., 1996). However, evidence for glucuronic acid metabolism in humans is indispensable for estimating the magnitude of drug–drug interactions between CYP2C8 substrates and candesartan acyl-β-D glucuronide in clinical settings. Oral administration of 1 mg/kg candesartan cilexetil resulted in 0.8% of candesartan acyl-β-D glucuronide excreted in feces 48 h after administration. In the same study, administration of 1 mg/kg of candesartan cilexetil [C^{14}] into the duodenum of rats through cannulated biliary tract resulted in excretion of candesartan acyl-β-D in feces 24 h after the administration, having [C^{14}] content that was 7.9% of the dose. Hence, candesartan acyl-β-D glucuronide likely undergoes deconjugation in the digestive tract and enters the enteric circulation as candesartan (Kondo et al., 1996), making it challenging to detect candesartan acyl-β-D glucuronide in humans.

UGT1A10 mRNA is not detectable in the human liver; however, UGT1A10 is predominantly expressed in the intestine. *UGT1A7*, *UGT1A8*, and *UGT1A9* mRNAs are

DMD Fast Forward. Published on January 14, 2021 as DOI: 10.1124/dmd.120.000126
This article has not been copyedited and formatted. The final version may differ from this version.

expressed at lower levels than *UGT1A10* in the intestine, while only *UGT1A7* and *UGT1A9* mRNAs are expressed in the liver (Ohno and Nakajin, 2009). Alonen et al. (2008) reported that UGT2B4, UGT2B10, UGT2B15, UGT2B17, and UGT2B28 do not contribute to the *O*-glucuronidation of candesartan. *UGT2B7* mRNA is expressed at a two-fold higher level in the intestine than *UGT1A10* (Ohno and Nakajin, 2009). Thus, UGT2B7 must contribute to the formation of candesartan acyl-β-D glucuronide in the liver. However, candesartan acyl-β-D glucuronide formation is more complex in the liver than in the intestine. Interestingly, following intravenous administration of ^{14}C-labeled candesartan *N2*-glucuronide, candesartan and candesartan acyl-β-D-glucuronide were detected in rat bile, whereas candesartan *N*2-glucuronide was not detectable (Kondo et al., 1996). Hence, candesartan acyl-β-D-glucuronide might be formed by transformation via acyl migration from *N*2-glucuronide to *O*-glucuronide or by enzymatic deconjugation via hydrolase, and subsequently reglucuronization by UGT2B7. Further studies are warranted to clarify the mechanism of candesartan acyl-β-D-glucuronide formation in the liver.

The absolute bioavailability of candesartan following oral administration of candesartan cilexetil, as a tablet or as an alcohol solution, is 15% (Product Monograph, AstraZeneca, Canada) and 42.3% (Yamaoka et al., 1981), respectively. The low absorption of candesartan is likely caused by the efflux transporter P-glycoprotein as well as by its low solubility (Satturwar et al., 2007). In closed-loop pharmacokinetic studies with naringin, a P-glycoprotein substrate, using an *in situ* rat model, Surampalli et al. (2015) reported a 1.34-fold increase in AUC, with an elevated peak concentration (C_{max}) of candesartan. However, naringin is also a strong inhibitor of UGT1A10 (IC_{50} value = 3.4 μM) (Gufford et al., 2014). UGT-mediated glucuronidation is reportedly an important detoxification pathway in the intestine for numerous endo- or xenobiotics, and is responsible for the first-pass pathway of several drugs, including raloxifene (Kemp et al., 2002), and phenolics (e.g., resveratrol, quercetin) (Wu et al., 2011). Cumulatively, these data may indicate that glucuronidation of candesartan in the intestine contributes to its low bioavailability.

DMD Fast Forward. Published on January 14, 2021 as DOI: 10.1124/dmd.120.000126
This article has not been copyedited and formatted. The final version may differ from this version.

We also identified candesartan glucuronides as substrates and moderate inhibitors of OATP1B1 and OATP1B3 (Fig. 3), compared with strong OATP1B1 inhibitors (i.e., cyclosporine, itraconazole, and rifampicin; Karlgren et al., 2012; McFeely et al., 2020). Specifically, at 10 μM, candesartan and acyl-β-D-glucuronide exhibited less than 50% inhibition of OATP1B1 and OATP1B3 (Fig. 4). Most drug interactions involving transporters depend on the unbound concentration of the drug. Indeed, 1 μM of candesartan was found to only slightly inhibit OATP1B1 and OATP1B3 with the estimated maximum total concentration ($[I]_{inlet,max}$, 0.52 μM) and maximum unbound concentration of candesartan in the liver inlet ($[I]_{u,inlet,max}$, 2.6 nM), calculated using the parameters (total hepatic blood flow rate = 97 L/h; unbound fraction (f_u) = 0.005; C_{max} = 0.22 μM (Hoogkamer et al., 1998); k_a = 1.485 h^{-1} (Meineke et al., 1997); dose = 12 mg of candesartan cilexetil; $F_a \times F_g = 1$ (Ito et al., 1998)), not reaching the inhibitory concentration. Conversely, candesartan glucuronides were only detectable in the bile acid (Kondo et al, 1996), while their hepatic concentrations remain unknown. Therefore, at the clinical dose, candesartan and its glucuronides are not likely to reach sufficient concentrations to inhibit OATP1B1 and OATP1B3. Hence, there is a low probability of drug–drug interactions occurring involving OATP1B1 and OATP1B3 upon oral administration of candesartan cilexetil.

Our results also demonstrated that candesartan *N*2-glucuronide and candesartan acyl-β-D-glucuronide serve as substrates of OATP1B1 and OATP1B3 (Fig. 3), which are important transporters for hepatic uptake of various drugs from the portal and systemic circulating blood. Specifically, candesartan acyl-β-D-glucuronide exhibited high affinity for OATP1B3 compared to candesartan *N*2-glucuronide (Fig. 3). Several researchers have reported unique pharmacokinetics of glucuronides. For instance, gemfibrozil acyl glucuronide, a potent CYP2C8 inhibitor, is a substrate of OATP1B1, with a higher affinity than gemfibrozil (Shitara et al., 2004). Sallustio et al. (1996) reported that the liver:perfusate concentration ratio of gemfibrozil acyl glucuronide is 35:42. Vasilyeva et al. (2015) reported that sorafenib glucuronide was barely detectable in mouse plasma, the liver-to-plasma ratio of sorafenib glucuronide was approximately 350 after oral sorafenib administration, and the ratio markedly

DMD Fast Forward. Published on January 14, 2021 as DOI: 10.1124/dmd.120.000126
This article has not been copyedited and formatted. The final version may differ from this version.

decreased in *Oatp1a/1b* knockout mice. Therefore, candesartan acyl-β-D-glucuronide may also accumulate at a high concentration in the liver. Kondo et al. (1996) further confirmed the enterohepatic circulation of candesartan using a radioisotope. Hence, following glucuronidation of candesartan in the intestine or hepatocytes, candesartan acyl-β-D-glucuronide might continuously accumulate in hepatocytes, being actively taken up by OATP1B1 and OATP1B3 and transported via the enterohepatic circulation, thereby facilitating its interaction with CYP2C8 substrates (Fig. 8).

In summary, candesartan acyl-β-D-glucuronide is converted into a strong CYP2C8 inhibitor, and functions as OATP1B1 and OATP1B3 substrate. Our findings suggest that following administration of candesartan cilexetil, candesartan acyl-β-D-glucuronide is actively transported by OATPs into hepatocytes, resulting in drug–drug interactions with CYP2C8 substrates, such as paclitaxel. These results provide new insights for considering the interaction between candesartan and paclitaxel in clinical practice, that cannot be explained solely by inhibition of the paclitaxel excretion pathway by candesartan. However, owing to the large differences in the metabolic profiles of humans, rats, and dogs, it remains unclear whether glucuronic acid metabolites identified in *in vivo* studies are physiologically relevant to these various organisms. Therefore, further clinical studies on the interaction between CYP2C8 substrate drugs and candesartan, as well as investigation into the metabolic profile of candesartan using human hepatocytes and small intestinal microsomes are needed.

DMD Fast Forward. Published on January 14, 2021 as DOI: 10.1124/dmd.120.000126
This article has not been copyedited and formatted. The final version may differ from this version.

Acknowledgments

We thank Prof. Kusuhara and Dr. Maeda (Laboratory of Molecular Pharmacokinetics, Tokyo University, Japan) for providing the HEK/OATP1B3 cells.

Authorship Contributions

Participated in research design: Katsube, Tsujimoto, Minegaki, and Nishiguchi

Conducted experiments: Katsube, Koide, and Minegaki

Performed data analysis: Katsube

Wrote or contributed to the writing of the manuscript: Katsube, Tsujimoto, Koide, Hira, Ikeda, Minegaki, Morita, Terada, and Nishiguchi

DMD Fast Forward. Published on January 14, 2021 as DOI: 10.1124/dmd.120.000126
This article has not been copyedited and formatted. The final version may differ from this version.

References

Agergaard K, Mau-Sørensen M, Stage TB, Jørgensen TL, Hassel RE, Steffensen KD, Pedersen JW, Milo MLH, Poulsen SH, Pottegård A, Hallas J, Brøsen K, and Bergmann TK (2017) Clopidogrel-Paclitaxel Drug-Drug Interaction: A Pharmacoepidemiologic Study. *Clin Pharmacol Ther* **102**:547–553.

Alonen A, Finel M, and Kostiainen R (2008) The human UDP-glucuronosyltransferase UGT1A3 is highly selective towards N2 in the tetrazole ring of losartan, candesartan, and zolarsartan. *Biochem Pharmacol* **76**:763–772.

Backman JT, Filppula AM, Niemi M, and Neuvonen PJ (2015) Role of Cytochrome P450 2C8 in Drug Metabolism and Interactions. *Pharmacological Reviews* **68**:168–241.

Backman JT, Kyrklund C, Neuvonen M, and Neuvonen PJ (2002) Gemfibrozil greatly increases plasma concentrations of cerivastatin. *Clin Pharmacol Ther* **72**:685–691.

Chang JT, Staffa JA, Parks M, and Green L (2004) Rhabdomyolysis with HMG-CoA reductase inhibitors and gemfibrozil combination therapy. *Pharmacoepidemiol Drug Saf* **13**:417–426.

Cresteil T, Monsarrat B, Dubois J, Sonnier M, Alvinerie P, and Gueritte F (2002) Regioselective metabolism of taxoids by human CYP3A4 and 2C8: structure-activity relationship. *Drug Metab Dispos* **30**:438–445.

De Bruyn T, Fattah S, Stieger B, Augustijns P, and Annaert P (2011) Sodium fluorescein is a probe substrate for hepatic drug transport mediated by OATP1B1 and OATP1B3. *J Pharm Sci* **100**:5018–5030.

Farid NA, Kurihara A, and Wrighton SA (2010) Metabolism and disposition of the thienopyridine antiplatelet drugs ticlopidine, clopidogrel, and prasugrel in humans. *J Clin Pharmacol* **50**:126–142.

Foti RS, Diaz P, and Douguet D (2016) Comparison of the ligand binding site of CYP2C8 with CYP26A1 and CYP26B1: a structural basis for the identification of new inhibitors of the retinoic acid hydroxylases. *J Enzyme Inhib Med Chem* **31**:148–161.

Fujino H, Yamada I, Shimada S, and Yoneda M (2001) Simultaneous determination of taxol

and its metabolites in microsomal samples by a simple thin-layer chromatography radioactivity assay--inhibitory effect of NK-104, a new inhibitor of HMG-CoA reductase. *J Chromatogr B Biomed Sci Appl* **757**:143–150.

Garg MB, and Ackland SP (2000) Simple and sensitive high-performance liquid chromatography method for the determination of docetaxel in human plasma or urine. *J Chromatogr B Biomed Sci Appl* **748**:383–388.

Gertz M, Tsamandouras N, Säll C, Houston JB, and Galetin A (2014) Reduced physiologically-based pharmacokinetic model of repaglinide: impact of OATP1B1 and CYP2C8 genotype and source of in vitro data on the prediction of drug-drug interaction risk. *Pharm Res* **31**:2367–2382.

Gufford BT, Chen G, Lazarus P, Graf TN, Oberlies NH, and Paine MF (2014) Identification of diet-derived constituents as potent inhibitors of intestinal glucuronidation. *Drug Metab Dispos* **42**:1675–1683.

Harris JW, Rahman A, Kim BR, Guengerich FP, and Collins JM (1994) Metabolism of taxol by human hepatic microsomes and liver slices: participation of cytochrome P450 3A4 and an unknown P450 enzyme. *Cancer Res* **54**:4026–4035.

Hoogkamer JF, Kleinbloesem CH, Ouwerkerk M, Högemann A, Nokhodian A, Kirch W, and Weidekamm E (1998) Pharmacokinetics and safety of candesartan cilexetil in subjects with normal and impaired liver function. *Eur J Clin Pharmacol* **54**:341–345.

Huizing MT, Sparreboom A, Rosing H, van Tellingen O, Pinedo HM, and Beijnen JH (1995) Quantification of paclitaxel metabolites in human plasma by high-performance liquid chromatography. *J Chromatogr B Biomed Appl* **674**:261–268.

Ito K, Iwatsubo T, Kanamitsu S, Ueda K, Suzuki H, and Sugiyama Y (1998) Prediction of pharmacokinetic alterations caused by drug-drug interactions: metabolic interaction in the liver. *Pharmacol Rev* **50**:387–412.

Jenkins SM, Zvyaga T, Johnson SR, Hurley J, Wagner A, Burrell R, Turley W, Leet JE, Philip T, and Rodrigues AD (2011) Studies to further investigate the inhibition of human liver microsomal CYP2C8 by the acyl-β-glucuronide of gemfibrozil. *Drug Metabolism and*

Disposition **39**:2421–2430.

Kajosaari LI, Laitila J, Neuvonen PJ, and Backman JT (2005) Metabolism of repaglinide by CYP2C8 and CYP3A4 in vitro: effect of fibrates and rifampicin. *Basic Clin Pharmacol Toxicol* **97**:249–256.

Karlgren M, Vildhede A, Norinder U, Wisniewski JR, Kimoto E, Lai Y, Haglund U, and Artursson P (2012) Classi fi cation of Inhibitors of Hepatic Organic Anion Transporting Polypeptides (OATPs): In fl uence of Protein Expression on Drug − Drug Interactions. *Journal of Medicinal Chemistry* **55**:4740–4763.

Katsube Y, Hira D, Tsujimoto M, Koide H, Minegaki T, Ikeda Y, Morita S, Nishiguchi K, and Terada T (2018) Concomitant administration of candesartan cilexetil in patients on paclitaxel and carboplatin combination therapy increases risk of severe neutropenia. *Int J Clin Pharmacol Ther* **56**:328–336.

Katsube Y, Tsujimoto M, Koide H, Ochiai M, Hojyo A, Ogawa K, Kambara K, Torii N, Shima D, Furukubo T, Izumi S, Yamakawa T, Minegaki T, and Nishiguchi K (2017) Cooperative inhibitory effects of uremic toxins and other serum components on OATP1B1-mediated transport of SN-38. *Cancer chemotherapy and pharmacology* **79**:783–789, Springer Berlin Heidelberg.

Kemp DC, Fan PW, Stevens JC, Carolina N, Toxicology C, Hill C, K NCDC, and Metabolism GD (2002) Characterization of Raloxifene Glucuronidation in Vitro : Contribution of Intestinal Metabolism To Presystemic Clearance Abstract : *Drug Metab Dispos* **30**:694–700.

Koide H, Tsujimoto M, Takeuchi A, Tanaka M, Ikegami Y, Tagami M, Abe S, Hashimoto M, Minegaki T, and Nishiguchi K (2017) Substrate-dependent effects of molecular-targeted anticancer agents on activity of organic anion transporting polypeptide 1B1. *Xenobiotica* 1–13.

Kondo T, Yoshida K, Yoshimura Y, Motohashi M, and Tanayama S (1996) Disposition of the new angiotensin II receptor antagonist candesartan cilexetil in rats and dogs. *Arzneimittelforschung* **46**:594–600.

Kumar S, Samuel K, Subramanian R, Braun MP, Stearns RA, Chiu S-HL, Evans DC, and Baillie TA (2002) Extrapolation of diclofenac clearance from in vitro microsomal metabolism data: role of acyl glucuronidation and sequential oxidative metabolism of the acyl glucuronide. *J Pharmacol Exp Ther* **303**:969–978.

Lassila T, Hokkanen J, Aatsinki S-M, Mattila S, Turpeinen M, and Tolonen A (2015) Toxicity of Carboxylic Acid-Containing Drugs: The Role of Acyl Migration and CoA Conjugation Investigated. *Chem Res Toxicol* **28**:2292–2303.

LOWRY OH, ROSEBROUGH NJ, FARR AL, and RANDALL RJ (1951) Protein measurement with the Folin phenol reagent. *J Biol Chem* **193**:265–275.

Ma S-F, Anraku M, Iwao Y, Yamasaki K, Kragh-Hansen U, Yamaotsu N, Hirono S, Ikeda T, and Otagiri M (2005) Hydrolysis of angiotensin II receptor blocker prodrug olmesartan medoxomil by human serum albumin and identification of its catalytic active sites. *Drug Metab Dispos* **33**:1911–1919.

Madan (2002) *Drug-drug interactions*, Volume 116.

McFeely SJ, Ritchie TK, Yu J, Nordmark A, Berglund EG, Levy RH, and Ragueneau-Majlessi I (2020) Inhibitors of Organic Anion-Transporting Polypeptides 1B1 and 1B3: Clinical Relevance and Regulatory Perspective. *Journal of Clinical Pharmacology*, doi: 10.1002/jcph.1604.

Meineke I, Feltkamp H, Högemann A, and Gundert-Remy U (1997) Pharmacokinetics and pharmacodynamics of candesartan after administration of its pro-drug candesartan cilexetil in patients with mild to moderate essential hypertension--a population analysis. *Eur J Clin Pharmacol* **53**:221–228.

Mitsuhiro N, Sudo M, Kawaguchi N, Takahashi J, Kiyota Y, Kondo T, and Asahi S (2012) An unusual metabolic pathway of sipoglitazar, a novel antidiabetic agent: cytochrome P450-catalyzed oxidation of sipoglitazar acyl glucuronide. *Drug Metab Dispos* **40**:249–258.

Ogilvie BW, Zhang D, Li W, Rodrigues AD, Gipson AE, Holsapple J, Toren P, and Parkinson A (2006) Glucuronidation converts gemfibrozil to a potent, metabolism-dependent

inhibitor of CYP2C8: implications for drug-drug interactions. *Drug Metab Dispos* **34**:191–197.

Ohno S, and Nakajin S (2009) Determination of mRNA expression of human UDP-glucuronosyltransferases and application for localization in various human tissues by real-time reverse transcriptase-polymerase chain reaction. *Drug Metab Dispos* **37**:32–40.

Orr STM, Ripp SL, Ballard TE, Henderson JL, Scott DO, Obach RS, Sun H, and Kalgutkar AS (2012) Mechanism-based inactivation (MBI) of cytochrome P450 enzymes: structure-activity relationships and discovery strategies to mitigate drug-drug interaction risks. *J Med Chem* **55**:4896–4933.

Sallustio BC, Fairchild BA, Shanahan K, Evans AM, and Nation RL (1996) Disposition of gemfibrozil and gemfibrozil acyl glucuronide in the rat isolated perfused liver. *Drug Metab Dispos* **24**:984–989.

Satturwar P, Eddine MN, Ravenelle F, and Leroux J-C (2007) pH-responsive polymeric micelles of poly(ethylene glycol)-b-poly(alkyl(meth)acrylate-co-methacrylic acid): influence of the copolymer composition on self-assembling properties and release of candesartan cilexetil. *Eur J Pharm Biopharm* **65**:379–387.

Senda A, Mukai Y, Toda T, Hayakawa T, Yamashita M, Eliasson E, Rane A, and Inotsume N (2015) Effects of Angiotensin II Receptor Blockers on Metabolism of Arachidonic Acid via CYP2C8. **38**:1975–1979.

Shitara Y, Hirano M, Sato H, and Sugiyama Y (2004) Gemfibrozil and its glucuronide inhibit the organic anion transporting polypeptide 2 (OATP2/OATP1B1:SLC21A6)-mediated hepatic uptake and CYP2C8-mediated metabolism of cerivastatin: analysis of the mechanism of the clinically relevant drug-drug interaction. *J Pharmacol Exp Ther* **311**:228–236.

Stierlin H, Faigle JW, Sallmann A, Küng W, Richter WJ, Kriemler HP, Alt KO, and Winkler T (1979) Biotransformation of diclofenac sodium (Voltaren) in animals and in man. I. Isolation and identification of principal metabolites. *Xenobiotica* **9**:601–610.

Surampalli G, K Nanjwade B, and Patil PA (2015) Corroboration of naringin effects on the

intestinal absorption and pharmacokinetic behavior of candesartan cilexetil solid dispersions using in-situ rat models. *Drug Dev Ind Pharm* **41**:1057–1065.

Taavitsainen P, Kiukaanniemi K, and Pelkonen O (2000) In vitro inhibition screening of human hepatic P450 enzymes by five angiotensin-II receptor antagonists. *Eur J Clin Pharmacol* **56**:135–140.

Takagi M, Sakamoto M, Itoh T, and Fujiwara R (2015) Underlying mechanism of drug-drug interaction between pioglitazone and gemfibrozil: Gemfibrozil acyl-glucuronide is a mechanism-based inhibitor of CYP2C8. *Drug Metab Pharmacokinet* **30**:288–294, Elsevier Ltd.

Tornio A, Filppula AM, Kailari O, Neuvonen M, Nyrönen TH, Tapaninen T, Neuvonen PJ, Niemi M, and Backman JT (2014) Glucuronidation converts clopidogrel to a strong time-dependent inhibitor of CYP2C8: a phase II metabolite as a perpetrator of drug-drug interactions. *Clin Pharmacol Ther* **96**:498–507.

Tornio A, Neuvonen PJ, Niemi M, and Backman JT (2017) Role of gemfibrozil as an inhibitor of CYP2C8 and membrane transporters. *Expert Opinion on Drug Metabolism and Toxicology* **13**:83–95.

Tsujimoto M, Uchida T, Kozakai H, Yamamoto S, Minegaki T, and Nishiguchi K (2016) Inhibitory Effects of Vegetable Juices on CYP3A4 Activity in Recombinant CYP3A4 and LS180 Cells. *Biol Pharm Bull* **39**:1482–1487.

van de Steeg E, Venhorst J, Jansen HT, Nooijen IHG, DeGroot J, Wortelboer HM, and Vlaming MLH (2015) Generation of Bayesian prediction models for OATP-mediated drug-drug interactions based on inhibition screen of OATP1B1, OATP1B1∗15 and OATP1B3. *Eur J Pharm Sci* **70**:29–36, Elsevier B.V.

Varma MVS, Lin J, Bi Y, Kimoto E, and Rodrigues AD (2015) Quantitative Rationalization of Gemfibrozil Drug Interactions: Consideration of Transporters-Enzyme Interplay and the Role of Circulating Metabolite Gemfibrozil 1-O-β-Glucuronide. *Drug Metab Dispos* **43**:1108–1118.

Vasilyeva A, Durmus S, Li L, Wagenaar E, Hu S, Gibson AA, Panetta JC, Mani S, Sparreboom

A, Baker SD, and Schinkel AH (2015) Hepatocellular Shuttling and Recirculation of Sorafenib-Glucuronide Is Dependent on Abcc2, Abcc3, and Oatp1a/1b. *Cancer Res* **75**:2729–2736.

Walsky RL, Gaman EA, and Obach RS (2005) Examination of 209 drugs for inhibition of cytochrome P450 2C8. *J Clin Pharmacol* **45**:68–78.

Wang J-S, Neuvonen M, Wen X, Backman JT, and Neuvonen PJ (2002) Gemfibrozil inhibits CYP2C8-mediated cerivastatin metabolism in human liver microsomes. *Drug Metab Dispos* **30**:1352–1356.

Wang Y, Wang M, Qi H, Pan P, Hou T, Li J, He G, and Zhang H (2014) Pathway-dependent inhibition of paclitaxel hydroxylation by kinase inhibitors and assessment of drug-drug interaction potentials. *Drug Metab Dispos* **42**:782–795.

Wu B, Kulkarni K, Basu S, Zhang S, and Hu M (2011) First-pass metabolism via UDP-glucuronosyltransferase: a barrier to oral bioavailability of phenolics. *Journal of pharmaceutical sciences* **100**:3655–81.

Yamaoka K, Tanigawara Y, Nakagawa T, and Uno T (1981) A pharmacokinetic analysis program (multi) for microcomputer. *J Pharmacobiodyn* **4**:879–885.

DMD Fast Forward. Published on January 14, 2021 as DOI: 10.1124/dmd.120.000126
This article has not been copyedited and formatted. The final version may differ from this version.

Footnote

All authors declare that: (i) no support, financial or otherwise, has been received from any organization that may have an interest in the submitted work; and (ii) there are no other relationships or activities that could appear to have influenced the submitted work.

DMD Fast Forward. Published on January 14, 2021 as DOI: 10.1124/dmd.120.000126
This article has not been copyedited and formatted. The final version may differ from this version.

Figure Legends

Fig. 1. Chemical structures of candesartan cilexetil and its metabolites.

Fig. 2. Kinetic analysis of candesartan glucuronidation to the *N*2-glucuronide (A and B) and acyl-β-D-glucuronide (C and D) form by human recombinant UGT1A10 and UGT2B7. (A and B) Candesartan *N*2-glucuronide levels were determined following incubation of the recombinant proteins (1.0 mg/mL) with UDPGA (5 mM) and candesartan (1–5 mM) at 37 °C for 60 min after a 5 min preincubation. (C and D) Candesartan acyl-β-D-glucuronide levels were determined following incubation of the recombinant proteins (0.5 mg/mL) with UDPGA (5 mM) and candesartan (30–1,000 μM) at 37 °C for 60 min after a 5 min preincubation. Each point represents the mean ± SD (n = 3).

Fig. 3. Kinetic analysis of candesartan *N*2-glucuronide (A) and acyl-β-D-glucuronide (B) uptake mediated by OATP1B1 and OATP1B3. The levels of candesartan *N*2-glucuronide and candesartan acyl-β-D-glucuronide were determined following

DMD Fast Forward. Published on January 14, 2021 as DOI: 10.1124/dmd.120.000126
This article has not been copyedited and formatted. The final version may differ from this version.

incubation of candesartan (0.5–30 μM) with HEK/OATP1B1 and HEK/OATP1B3 cells at 37 °C for 1 min after a 5 min preincubation. The K_m and V_{max} values were determined from a Michaelis–Menten plot using the MULTI program. Each point represents the mean ± SD (n = 4). The K_m and V_{max} values represent the estimate with 95% CI.

Fig. 4. Effects of candesartan and its glucuronides on the uptake of OATP1B1 and OATP1B3 probe substrates. (A) OATP1B1-mediated uptake of 2′,7′-dichlorofluorescein (DCF) was determined following incubation of DCF (5 μM) in the absence (control) or presence of candesartan (1 or 10 μM), candesartan *N*2-glucuronide (1 or 10 μM), or acyl-β-D-glucuronide (1 or 10 μM) with HEK/OATP1B1 cells. (B) OATP1B3-mediated uptake of FL was determined following incubation of fluorescein (FL; 2 μM) in the absence (control) or presence of candesartan (1 or 10 μM), candesartan *N*2-glucuronide (1 or 10 μM), or acyl-β-D-glucuronide (1 or 10 μM) with HEK/OATP1B3 cells. Each point represents the mean ± SD (n = 4). The significance of any differences from the control was determined by ANOVA, followed by the Dunnett's test (*p < 0.01, **p < 0.001).

DMD Fast Forward. Published on January 14, 2021 as DOI: 10.1124/dmd.120.000126
This article has not been copyedited and formatted. The final version may differ from this version.

Fig. 5. Effects of candesartan and candesartan glucuronides on hydroxylation of paclitaxel by CYP2C8 (A) and CYP3A4 (B). CYP2C8 and CYP3A4 activities were determined by hydroxylation of paclitaxel to 6α-hydroxypaclitaxel and *p*-3′-hydroxypaclitaxel, respectively. Hydroxylation was determined by incubation of the recombinant proteins (CYP2C8, 10 pmol/mL; CYP3A4, 10 pmol/mL) and paclitaxel (2 and 4 μM, respectively) with the NADPH-regenerating system at 37 °C for 30 min after a 5 min preincubation. Each point represents the mean ± SD (n = 3).

Fig. 6. An IC_{50} shift assay for time-dependent inhibition of CYP2C8 by preincubation with NADPH and candesartan acyl-β-D-glucuronide. CYP2C8 activity was determined by hydroxylation of paclitaxel to 6α-hydroxypaclitaxel. Hydroxylation was determined by incubation of human liver microsomes (HLMs; 0.1 mg protein/mL), with or without the initial addition of the NADPH-regenerating system, at 37 °C for 30 min. The mixture was added to paclitaxel (2 μM) and incubated for 10 min. Each point represents the mean ± SD (n = 3).

DMD Fast Forward. Published on January 14, 2021 as DOI: 10.1124/dmd.120.000126
This article has not been copyedited and formatted. The final version may differ from this version.

Fig. 7. Determination of K_i values for CYP2C8 inhibition by candesartan and candesartan acyl-β-D-glucuronide. The activity of CYP2C8 was determined based on hydroxylation of paclitaxel to 6α-hydroxypaclitaxel. Hydroxylation was determined by incubation of recombinant CYP2C8 (10 pmol/mL), test compounds (candesartan, 15.6–250 μM; candesartan acyl-β-D-glucuronide, 3.8–60 μM), and paclitaxel (0.5, 1.0, and 2.0 μM) with the NADPH-regenerating system at 37 °C for 30 min after a 5 min preincubation. Each point represents the mean ± SD (n = 3).

Fig. 8. Hypothesized mechanism for the potential drug interaction of candesartan cilexetil with paclitaxel. Hypothesized mechanism for the potential drug interaction of candesartan cilexetil with paclitaxel. Nearly all orally administered candesartan cilexetil becomes hydrolyzed to candesartan in the intestine, followed by glucuronidation to candesartan acyl-β-D-glucuronide by UGT1A10 and UGT2B7. Thereafter, candesartan acyl-β-D-glucuronide is actively transported into hepatocytes by OATP1B1 and OATP1B3. Candesartan is also transformed to acyl-β-D-glucuronide by UGT2B7 in the

liver, and glucuronides are secreted in the bile and reabsorbed through enterohepatocyte circulation. This cycle may result in an interaction between a CYP2C8 substrate and candesartan acyl-β-D-glucuronide. Acyl glu, candesartan acyl-β-D-glucuronide; BCRP, breast cancer resistance protein; CYP, cytochrome P450; MRP, multidrug resistance protein; OATP, organic anion-transporting polypeptide; UGT, UDP-glucuronosyltransferase.

DMD Fast Forward. Published on January 14, 2021 as DOI: 10.1124/dmd.120.000126
This article has not been copyedited and formatted. The final version may differ from this version.

Tables

Table 1. Inhibition of CYP2C8 and CYP3A4 by candesartan and its glucuronides, as related to paclitaxel metabolism.

Metabolite	CYP2C8		CYP3A4	
	IC_{50} (μM)	95% CI	IC_{50} (μM)	95% CI
Candesartan	150	123–176	> 250	
*N*2-glucuronide	166	135–197	191	125–257
Acyl-β-D-glucuronide	18.9	18.2–19.7	159	145–172

95%CI, confidence interval; IC_{50}, 50% inhibitory concentration (each value represents the mean).

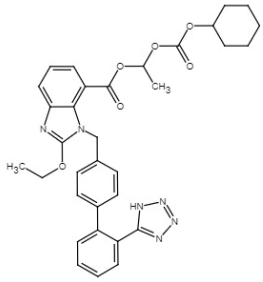

Candesartan cilexetil

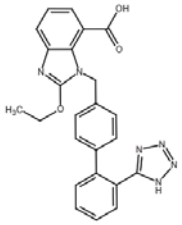

Candesartan

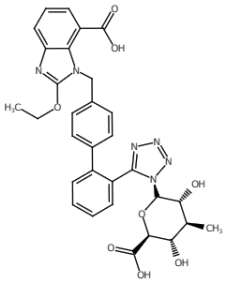

Candesartan *N*2-glucuronide

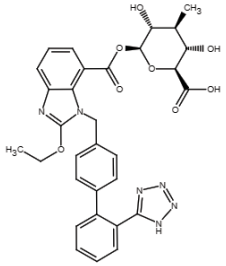

Candesartan acyl-β-D-glucuronide

Fig. 1

DMD Fast Forward. Published on January 14, 2021 as DOI: 10.1124/dmd.120.000126
This article has not been copyedited and formatted. The final version may differ from this version.

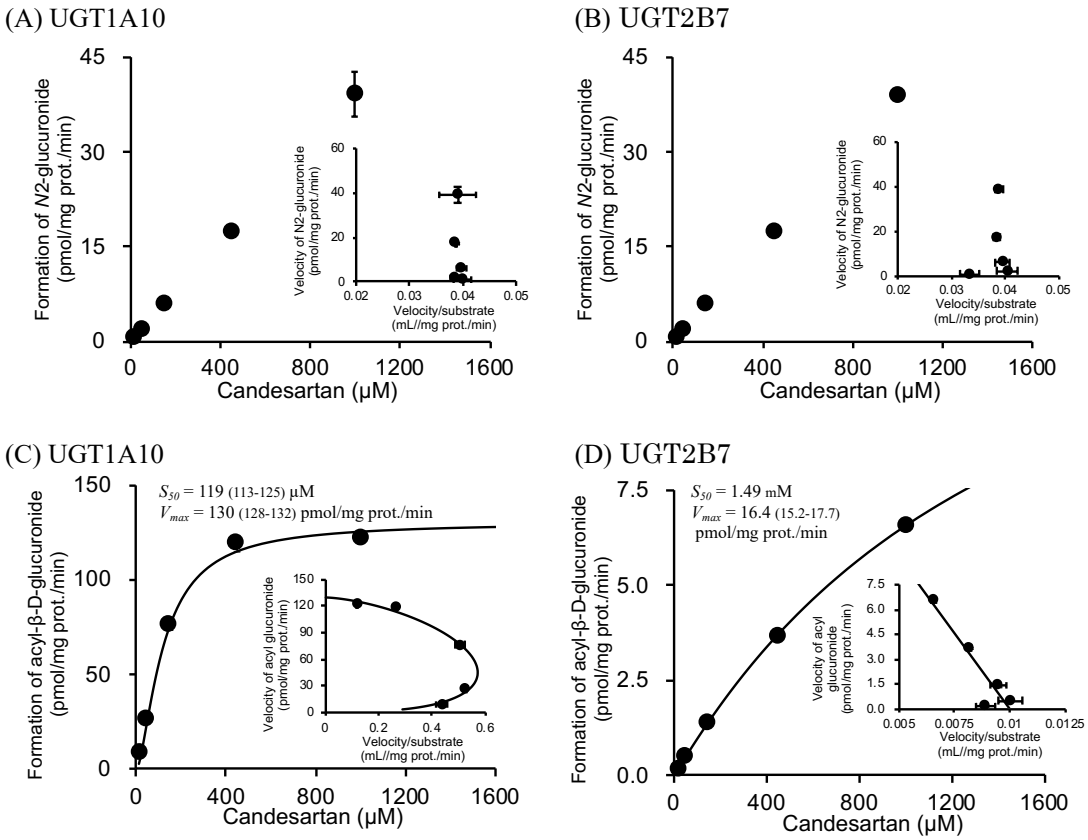

Fig. 2

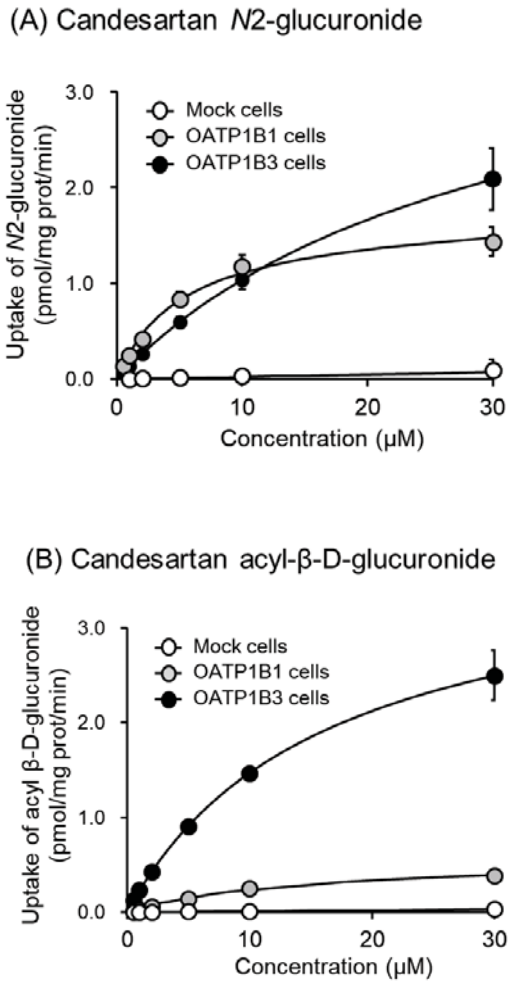

Fig. 3

(A) OATP1B1

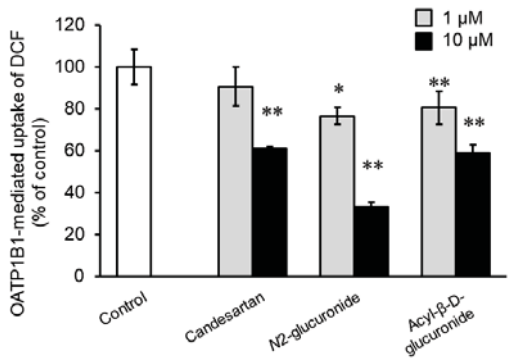

(B) OATP1B3

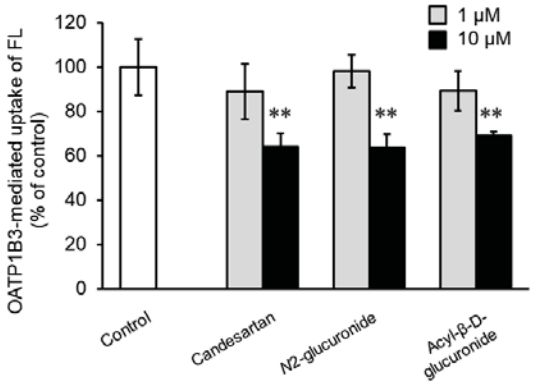

Fig. 4

DMD Fast Forward. Published on January 14, 2021 as DOI: 10.1124/dmd.120.000126
This article has not been copyedited and formatted. The final version may differ from this version.

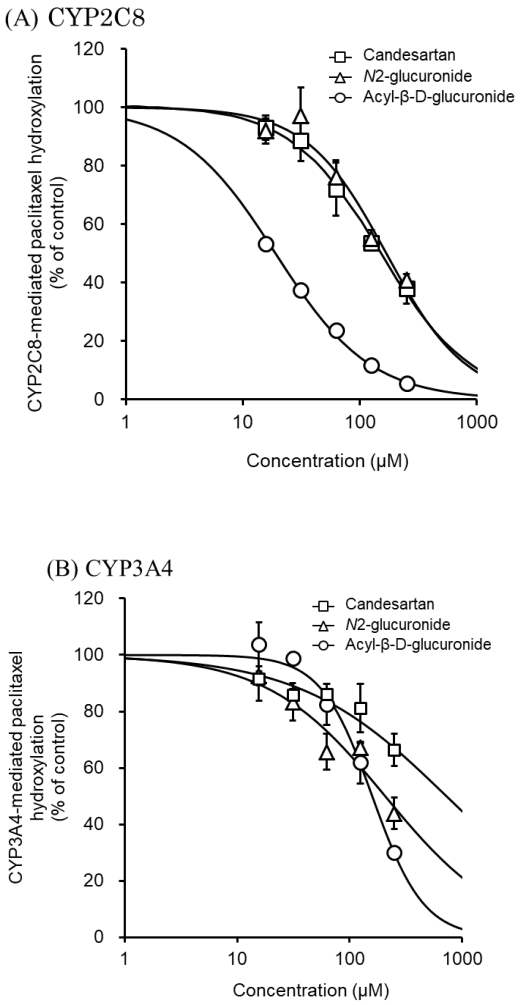

Fig. 5

DMD Fast Forward. Published on January 14, 2021 as DOI: 10.1124/dmd.120.000126
This article has not been copyedited and formatted. The final version may differ from this version.

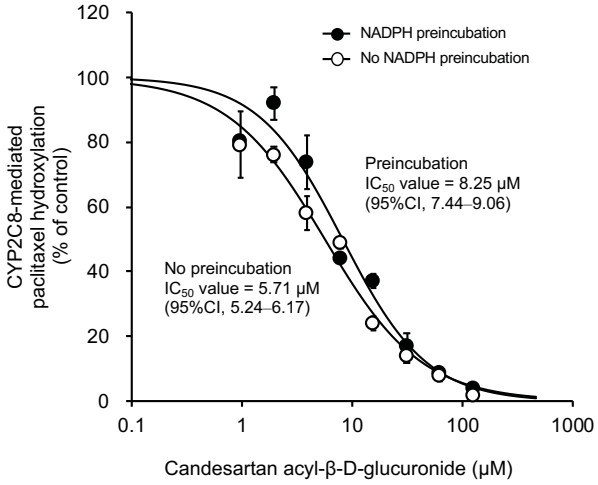

Fig. 6

(A) Candesartan

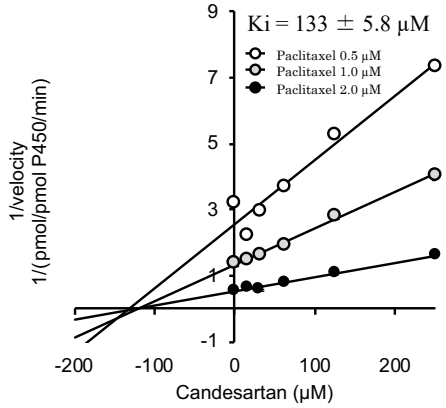

(B) Candesartan acyl-β-D-glucuronide

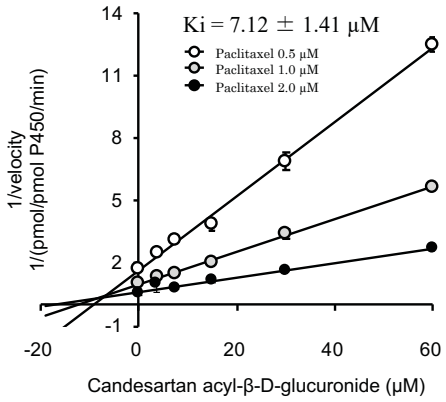

Fig. 7

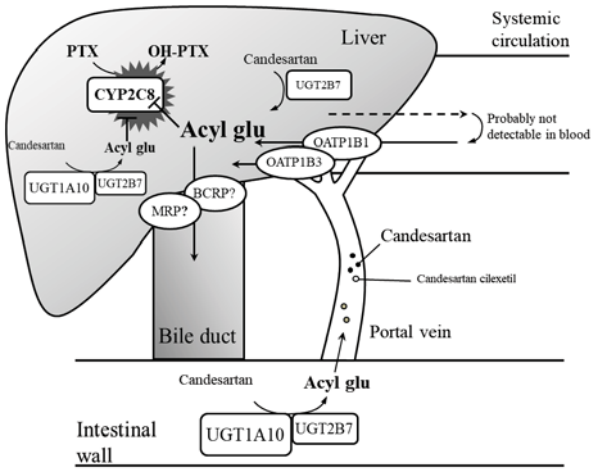

Fig. 8